

Introducing scale factor adjustments on agent-based simulations of the immune system

Juan A. Sánchez-Lantaron, Pedro A. Reche
 School of Medicine, Unit of Immunology,
 Complutense University of Madrid
 Madrid, Spain
parecheg@med.ucm.es

Giulia Russo
 Dept. of Biomedical and Biotechnological Sciences
 University of Catania
 Catania, Italy
giulia.russo@unict.it

Marzio Pennisi
 Dept. of Mathematics and Computer Science
 University of Catania
 Catania, Italy
mpennisi@dmi.unict.it

Francesco Pappalardo
 Dept. of Drug Sciences
 University of Catania
 Catania, Italy
francesco.pappalardo@unict.it

Juan A. Sánchez-Lantaron, Giulia Russo, Marzio Pennisi, Francesco Pappalardo, Pedro A. Reche

Corresponding authors: Francesco Pappalardo, Pedro A. Reche

Abstract— Immune system processes can be simulated using both system dynamics (SD) models based on differential equations and Agent-based (AB) models. The two approaches are intrinsically different but some methodologies have been developed to convert SD models into AB models with a variable degree of success. However, until now none of such methods have considered the use of scale factors in SD to AB model conversion. In this work, we revisited a well know SD model describing the interaction between effector T cells and tumor cells that was previously shown unsuitable for AB modeling. We introduced non-dimensional scaling factors in AB modeling and compared AB and AD simulations through a sensitivity analysis. Under this scenario, we obtained AB models that could successfully reproduce SD simulations with a reasonable number of agents and a stochastic behavior that did not compromise computer resources. In general, our results justify the introduction of non-dimensional scaling factors to reproduce SD simulations with AB models.

Keywords—artificial immune system; immune modeling; immunotherapy

I. INTRODUCTION

The immune system consists of a network of organs, tissues, cells and molecules whose main function is to protect the body from infection caused by pathogens. However, it is now reckoned that the immune system is also involved in tumor immunosurveillance [1] and more generally in maintaining body integrity and homeostasis [2, 3]. It relies on vast and diverse numbers of cells and molecules, has cognition and memory and interacts with the environment, mounting different types and intensities of responses.

As knowledge of the immune system grows it becomes increasingly clear that most of its actions/responses (eg. aggression, tolerance, suppression or tissue repair) emerge from integrated and complex networks of interactions involving multiple cells and molecules. Thereby, the experimental study of immune responses can be challenging or unviable and one needs to resort to mathematical modeling and/or computer model simulations [4-8].

There are many approaches to model and simulate immune processes. Arguably, system dynamics (SD) simulations based on ordinary differential equations (ODE) are the most widely used. To mention a few examples, ODE models have been applied to describe/simulate B and T cells responses [9-12], T cell dynamics [13, 14] and cancer immunology [15-19]. ODE models are simple and sound and have been thoroughly applied in the study of many biological, physical, chemical and engineering problems [18]. Moreover, ODE-models can get extremely complex before becoming unfeasible for finding solutions through computational simulations. However, SD simulations based on ODE-models do not capture spatial dynamics or stochastic effects, which are so inherent to the immune system [5, 18]. These properties can however be taken in consideration using Agent Based models (ABMs) [4, 5, 19].

Unlike differential equations, which deal with collective populations, ABMs simulate discrete and distinguishable agents, such as individual cells or molecules, and consider that the behavior of complex systems emerge out and can be modeled from interacting but autonomous learning agents. In addition, ABMs can easily account for the probabilistic uncertainty, stochasticity of biological systems [20, 21]. Despite being relative new, ABMs have been thoroughly used in immune system simulations [22], including antigen recognition by T cells [23], T cell motility in lymph nodes [24], B cell selection in germinal centers [23] and cancer immunity [25], just to cite a few examples. Moreover, there are also informatics packages specifically designed for ABM immune simulations such as the immune system simulator (IMMSIM) [26], the synthetic immune system (SIS) [27], the basic immune simulator (BIS) [28]. ABMs can capture more complex structures and dynamics than SD simulations but consume much more computational resources [5]. Nonetheless, in recent years huge increases in computer power have led to a growth in the use of ABMs. Moreover, there are rules and translation steps to convert SD models and ABMs. In fact, it is much easier to build an AB model if there is an SD model that already answer a specific question [5, 29]. However, ABM translations of existing SD models do not always match. Thus, Figueredo et al. [30] obtained similar results for a naive T cell output model using SD

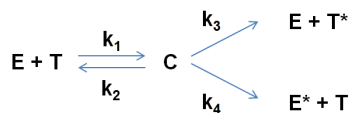
simulations and ABMs. However, for an ODE-model describing the interaction of effector T cell and tumor cells [31], Figueredo et al [32] found significant differences between the results produced by the SD simulations (SDS) of the ODE-model and the translated ABM.

In this work, we revisited the ABM conversion of the ODE-model depicting the interaction of effector T cells and tumor cells [31] using the same methodology of Figueredo et al [32], but introducing non-dimensional scaling factors prior to ABM conversion. We show that real problem parameters can be recovered after simulations and prove that in this non-dimensional space, ABM simulations get much closer to the SD solution.

II. SYSTEMS AND METHODS

A. Mathematical Model of the interaction between T cells and tumor cells

Effector T cells play key role in cancer immunosurveillance. In particular, Cytotoxic T lymphocytes (CTLs), detect and kill tumor cells. In this work, we used Kuznetsov et al [15] simple model to describe the interaction between effector T cells (E) and tumor cells (T), that is:



In this model, T cells engage (E) tumor cells (T) with possible outcomes that is: a) tumor cells are killed and effector cells can engage new T cells; b) tumor cells survive and effector cells are inactivated. These possible outcomes are governed by nonnegative kinetic constants k_1, k_2, k_3, k_4 . Under this model the variation in the concentration of species E and T is governed by the following equations:

$$\frac{dE}{dt} = s + \frac{pET}{g+T} - mET - dE \quad (1)$$

$$\frac{dT}{dt} = aT(1 - bT) - nET \quad (2)$$

Here, s represents an external influx of effector cells to the location of tumor cells; $\frac{pET}{g+T}$ represents the proliferation of effector cells; mET represents the number of effector cells killed by tumour cells; dE represents the death (apoptosis) of effector cells; $aT(1 - bT)$ represents the proliferation of tumour cells; nET represents the number of tumour cells killed by effector cells. Each one of the parameters can be estimated from experimental data, based on the growth dynamics of a BCL₁ lymphoma in the spleen of chimeric mice [33, 34], which has been used as a model for the lymphocytic leukemia in humans [35]. Taking into account initial values for the following parameters:

- $a = 0.18 \text{ day}^{-1}$
- $b = 2.0 \times 10^{-9} \text{ cells}^{-1}$
- $s = 1.3 \times 10^4 \text{ cells} \cdot \text{day}^{-1}$

the other parameters have been estimated taking into account experimental data gathered in [33] and [34]:

- $p = 0.1245 \text{ day}^{-1}$
- $g = 2.019 \times 10^7 \text{ cells}$
- $m = 3.422 \times 10^{-10} \text{ day}^{-1} \cdot \text{cells}^{-1}$
- $n = 1.101 \times 10^{-7} \text{ day}^{-1} \cdot \text{cells}^{-1}$
- $d = 0.0412 \text{ day}^{-1}$

B. Non-dimensionalization of the mathematical model

Mathematical models allow to predict the behavior of complex system by means of analyzing the equations outcome as a function of the initial values of the critical parameters. For a given mathematical model, it is a normal practice to non-dimensionalize the equations in order to take advantage of the following properties of the non-dimensionalization: *i)* unit absence that is, results are independent of the units of measurement; *ii)* equation optimization, in which the number of the equation parameters is reduced to the minimum; *iii)* similarity, in which equations results only depend of the non-dimensional parameter values, which are a combination of the initial parameters; *iv)* scale identification i.e., non-dimensional parameters allow the identification of the small parameters that could be ignored or treated approximately; *v)* scale definition that depends on the non-dimensional initial parameters, and final results can be scaled to the appropriate values. The number of non-dimensional parameters that can be generated for a given set of equations can be evaluated, as a function of the initial number of parameters and the number of dimensions used in the equations. Way forward to obtain this number is covered by the Buckingham Pi Theorem, which only defines the number of non-dimensional parameters but it does not define the specific parameters to be used, therefore several set of non-dimensionalized equations can be generated.

If (1) and (2) are non-dimensionalized, considering as non-dimensional parameters the scale of the effector and tumor cell population, E_0 and T_0 respectively, and the rate of tumor cells killed by each effector cells (parameter n) [15], then the equations can be re-expressed as:

$$\frac{dX}{d\tau} = \sigma + \frac{\rho XY}{\eta + Y} - \mu XY - \delta X \quad (3)$$

$$\frac{dT}{d\tau} = \alpha Y(1 - \beta Y) - XY \quad (4)$$

Where:

$$\begin{cases} X = \frac{E}{E_0}, Y = \frac{T}{T_0}, \tau = nT_0 t \\ \alpha = \frac{a}{nT_0}, \beta = bT_0, \sigma = \frac{s}{nE_0T_0} \\ \mu = \frac{m}{n}, \eta = \frac{mg}{nT_0}, \delta = \frac{d}{nT_0}, \rho = \frac{p}{nT_0} \end{cases} \quad (5)$$

Considering the scale factors for the effector and tumor cells population of:

$$E_0 = T_0 = 10^6 \text{ cells} \quad (6)$$

and the initial values of the parameters of (1) (2), resulting values for the non-dimensional parameters are the following:

$$\begin{cases} \alpha = 1.636, \beta = 2.0 \times 10^{-3}, \sigma = 0.1181 \\ \mu = 0.00311, \eta = 20.19, \delta = 0.3743, \rho = 1.131 \end{cases} \quad (7)$$

C. Non dimensional equations solution

If the system of (3) and (4) is solved numerically, by means of an Euler numerical method, considering as the initial values for the non-dimensional populations for the effector and tumor cell of $X_i = 4$ and $Y_i = 120$, and an integration step of $\Delta t = 0.01$, the outcome of the cell population temporal evolution is similar to the plot of Figure 1.

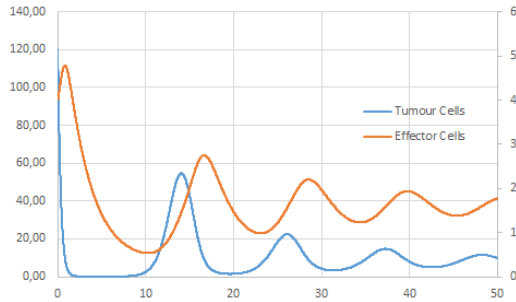


Figure 1. Numeric solution for non-dimensional effector and tumor cell interaction.

In Figure 1, in which the non-dimensional tumor cell population corresponds to the left axis, and the non-dimensional effector cell populations corresponds to the right axis, a predator-prey tendency can be appreciated, thus every time the tumor cells start to grow up, the effector cells also increases to mitigate the effect of the tumor cells, and after several oscillations, there is a tendency to one stationary point in which the effector cells can control the tumor cells populations in a so called dormant tumor state. It shall be noted that axes values only represent non-dimensional values. This is the reason why for a given time frame of the numerical solution, the non-dimensional tumor cells population is getting close to 0,0449 and the non-dimensional effector cells population oscillates during all the simulation between 1 and 3. For a real system, it will not make too much sense to have only 0.0449 cells of a given population, but from a non-dimensional point of view, this number may imply to have several hundreds of “living” cells in the system. Therefore, this is one important advantage of the SDS and its numerical solution, because this kind of equations supports any mathematical value for the cells population along its numerical solution.

D. Re-dimensioning of the system

Once the set of equations has been solved, with the purpose of analyzing the real outcomes of the solution, it is possible to recover physical units from the non-dimensional solution, using the relationship between the dimensional and non-dimensional parameters, described in (5). The equations outcome with physical units have been plotted in Figure 2.

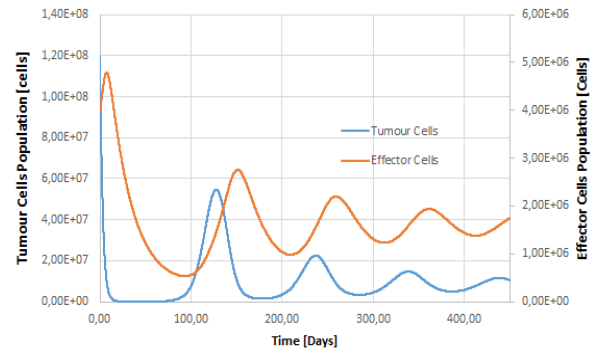


Figure 2. Numeric solution for effector and tumor cell interaction – physical units

For this particular case, tumor – effector cells tendency indicates that: *i)* minimum tumor cells population predicted by SDS is around 45.000 cells; *ii)* minimum effector cells population predicted by SDS is around 536.000 cells; *iii)* time frame necessary to achieve stationary conditions is higher than 450 days; *iv)* frequency of the population oscillations is close to 106 days.

E. Scale factors for non-dimensionalization of the equations

Scale factors selected for the evaluation of the equation parameters in (7) are arbitrary, and does not obey to any rule, apart from the goal of managing numbers within a fixed range for each cells population. Therefore, many scale factors can be used, obtaining the very same behavior for the cells populations, but with different non-dimensional value. To compare the benefit of managing different scale factors, four different scenarios, captured in Table 1, have been solved. Each scenario has different scale factors (E_0 , T_0 and t_0), therefore the non-dimensional parameters values will be different, having thus an impact in the range of the outcome for the different non-dimensional cells populations.

TABLE I. SCALE FACTORS USED IN EACH SCENARIO TO SOLVE NON-DIMENSIONAL EQUATIONS (3) (4)

Scenario	Scale Factors			Non-dimensional Parameters							Initial Conditions	
	E_0	T_0	t_0	α	β	σ	μ	η	δ	ρ	X_i	Y_i
a	10^6	10^6	1	1.636	2×10^{-3}	0.1181	3.11×10^{-3}	20.19	0.3743	1.131	1.2×10^7	4
b	10^6	10^4	1	1.636	2×10^{-3}	11.81	3.11×10^{-3}	20.19	0.3743	1.131	1.2×10^7	400
c	10^6	10^3	1	1.636	2×10^{-6}	118.1	3.11×10^{-6}	20.19	0.3743	1.131	1.2×10^7	4000
d	10^6	10^4	1/2	0.818	2×10^{-3}	5.905	1.55×10^{-3}	20.19	0.187	0.566	1.2×10^7	400

Plots for the numerical solutions of the four scenarios gathered in Table 1 have been compiled in Figure 3. Comparing four plots, it can be stated that the evolution of the cells population in all the cases follows the same pattern. Main difference between all of them relays in the scale of the axis. In particular, for the first three scenarios (a, b and c), non-dimensional time scale (horizontal axis) is an invariant, and only the scale of both cells population is affected. In the fourth chart (d), the time scale has been reduced to the half, and therefore the evolution is slower than in the other three scenarios, being necessary to extend the numerical integration twice times, to be able to reproduce the same behavior as in the previous scenarios.

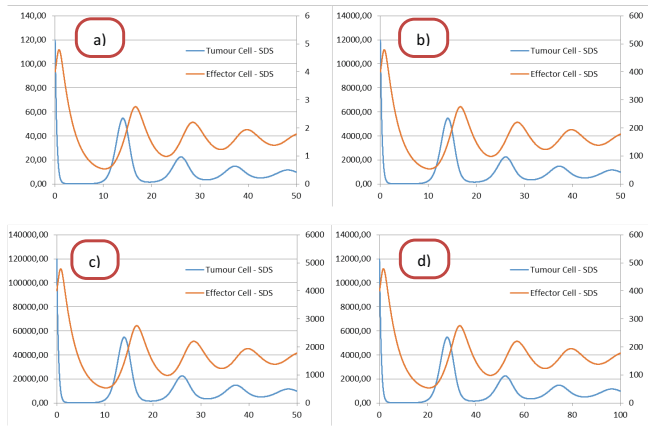


Figure 3. Non-dimensional cells population evolution for the four scenarios captured in Table 1.

In all the scenarios, if the scale factor decreases, the range of cells population will increase. In fact, if the scale factors are 1, number of cells population will be similar to the real number of cells involved in the solution of the dimensional equations. As the cells population range varies with the scale factors, it is interesting to analyze minimum and maximum values achieved during the simulation, because these numbers will be the critical parameters to be taken into account to select the best AB Simulation (ABS) option. These maximum and minimum values obtained for the non-dimensional cells populations and the non-dimensional time have been captured in Table 2. It is important to highlight that, varying the scale factors, it is possible to size the equations in order to have a minimum number of tumor and effector cells higher than 1, which is a very important point in order to translate this kind of problem to a ABS problem.

TABLE II. MAXIMUM AND MINIMUM VALUES FOR THE NON-DIMENSIONAL CELL POPULATIONS AND NON-DIMENSIONAL TIME ACHIEVED DURING THE NUMERICAL INTEGRATION OF SCENARIOS GATHERED IN TABLE I

Scenario	Tumour Cells		Effector Cells		Time	
	Max value	Min value	Max value	Min value	Max value	Min value
a	120	0.04	4.79	0.54	0	50
b	12000	4.49	479.02	53.57	0	50
c	120000	44.93	4790.15	535.67	0	50
d	12000	4.49	479.02	53.57	0	100

As it was done for the first example, the physical units can be recovered from the non-dimensional plots, being the final solution equal for all of the four scenarios, and being equal to the plot captured in Figure 2, because the four scenarios analyzed covered the solution to the physical problem described through equations (1) and (2). From the analysis of the result for the fourth scenarios compiled in Table 1, it appears that for a given set of differential equations, a non-dimensional set of equations can be generated through specific grouping of the dimensional parameters. Non-dimensional parameters can be scaled by means of dedicated scale factors without impacting in the equation results behavior. If the scale factor increases, the maximum and minimum values of non-dimensional cell

population decrease in the same proportion. Scaling factors can be applied to both axes independently (time axis and cell population axis). Physical solution can be recovered, independently of the scale factors used during the non-dimensionalization process of the equations.

F. ABS model generation from the SDS

ABS technique is a modelling approach that works with autonomous entities (agents), with the purpose of simulating dynamics of complex systems. Actions and interactions among different agents are defined by rules imposed to each agent. Despite the model is focused in the agents, ABS provides outcomes that allows to predict the behavior of the agents as a global entity rather than focus only on particular agent behaviors, creating an emergent order. The state charts identify each one of the different possible states of an entity, and define the events that can be triggered to change current agent state to another. State charts for this particular interaction between the effector cells and tumour cells has been already analyzed in [32] and [38], and for this study, the state charts considered are shown in Figure 4.

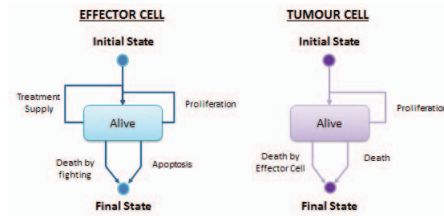


Figure 4. Effector cells and Tumour cell state charts.

Transition rates for each one of the transitions covered in the states charts are defined from the non-dimensional equations (3) and (4) and they have been compiled in Table 3. It shall be noted that transition rates compiled in this table, are the parameters of the equations (3) and (4) but defined per cell population, as the transitions shall be imposed per agent unit.

TABLE III. TRANSITION RATES FOR EACH EFFECT AND TUMOUR CELL AGENTS TRANSITIONS DEFINED IN FIGURE 4

Effector Cell Transition Rates		Tumour Cell Transition Rates	
Treatment Supply	σX	Proliferation	α
Proliferation	$\rho Y \eta + Y$	479.02	$\alpha \beta Y$
Death by fighting	μY	Death by Effector Cell	X
Natural Apoptosis	δ		

G. Case of study

ABS modelling cannot be used to solve systems models whose variables can have values lower than one, as this kind of modelling manages discrete entities, and therefore every time that one agent population falls below 0 implies that such agent will disappear from the simulation.

Non-dimensionalization process defined for the SDS can be translated to the ABS model, by means of adjusting the transition rates gathered in Table 3, considering different values for the scale factors defined in (6). Non-dimensionalization can be

understood as a cell grouping process in packs, where the behavior of each pack is defined for the behavior of its equivalent non-dimensional entity. Therefore, the scale factor represents the number of cells that are packed together, so for a given cell population, if the scale factor increases, the number of non-dimensional entities decrease, and in the other hand lower scale factors will imply to increase the number of non-dimensional entities.

This equivalence allows to simulate the real scenario through a non-dimensional system based on entities behavior that represents a pack of cells. Therefore, in the first case analyzed, where: *i)* scale factor: $E_0 = T_0 = 10^6$ cells, *ii)* non-dimensional initial values of the effector and tumor cells population: $X_i = 4$ and $Y_i = 120$. The initial tumor cell population of 1.2×10^8 cells has been approached with 120 packs, of 10^6 cells in each pack, and the effector cell population of 4×10^6 cells has been approached with 4 packs, of 10^6 cells in each pack. This approach has the benefit of reducing the computer resources, as the number of entities to be simulated are reduced drastically, but in the other way stochastic effects have a higher influence when the number of entities is too low. In this particular case, as the non-dimensional population of effector cells is 4, a slight fluctuation around of this value, due to the stochastic effects, will originate an unexpected extinction of this population. Although the above example has been focused on the effect of the scale factor in the cell population, it shall be highlighted that this process can be applied also to the time. Therefore, the scale factor adjustment can help to optimize computer resources for the simulation of ABS models, but may introduce some stochastic effects that are not present in the real system. Therefore, along this paper a sensitivity analysis of the ABS outcome with the scale factor will be performed in order to understand what is the maximum scale factor that can be used to maintain similar outputs than for the SDS. Additionally, time necessary to perform each simulation will be recorded to study the effect of the scale factors.

H. ABS solution algorithm

To evaluate temporal evolution of the agents, a complete ABS algorithm has been built, considering the state charts for the cells populations described in Figure 4, and the transition rates defined in Table 3. The proposed model is discrete in time, so, in each time step, agent states and transition will be evaluated by means of a particularization of the Gillespie's algorithm, in which, instead of applying the algorithm for each one of the reactions in which can be split the differential equations, this algorithm is applied to determine the transition triggered by each agent, and the time necessary to trigger such transition. In particular we fix the time step Δt as the model is discrete in time, so transition rates will remain constant during each time step, being these values refreshed at the beginning of each iteration. For each agent, time necessary to trigger a transition, τ , is controlled by the following exponential probabilistic function:

$$\tau = \frac{1}{\theta_0} \text{Ln} \left[\frac{1}{r_1} \right] \quad (8)$$

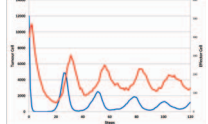
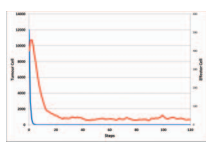
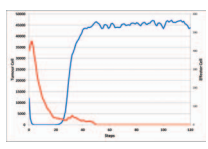
where θ_0 represents the sum of all the transitions rates for a given population and r_1 is a random number between 0 and 1. In each time step, the time needed to trigger a transition, τ , is compared with the time step duration. If $\tau \leq \Delta t$ then the

transition is triggered during that particular timestep; if $\tau > \Delta t$ then the transition is not triggered, and population of that agent will not be modified. Once that τ has been defined, transition carried out is selected randomly between all the potential transition for each agent, based on a second random number (r_2), considering the different transition rates as weights in comparison with θ_0 . If the transition triggered does not imply the death of the agent, a new evaluation for the time needed to trigger a new transition is performed, to cover those transitions that may be triggered in one agent more than once time per each time step. If the transition implies a birth of a new agent, time for the next transition is also evaluated for the new born agents, to take into account any potential transition that may be triggered in these new agents, between the birth time and the end of the time step. At the end of each time step, total agent population is recorded and transitions rates are updated to start the evaluation of the next time step.

III. RESULTS

Results obtained for the sensitivity analysis performed to determine the influence of the cell population scale factors in the outcomes of the ABS have been captured in Figure 5 and Figure 6. All the plots capture the 500 runs for each case study, and for reference purposes, each plot includes the average value of these 500 runs, and the SDS solution. Additionally, Figure 5 and Figure 6 also include the representation of the mean value of each simulation, once the dimensional values for each axis has been recovered. Due to the stochastic effect of the ABS model, three different patterns for the model outcome have been detected during all the simulations, as shown in Table 4.

TABLE IV. CELLS POPULATION PATTERNS DETECTED DURING ABS SIMULATIONS

<ul style="list-style-type: none"> • Case 1 - SDS behavior: Tumor and effector cell populations never decays under the minimum value of 1, and therefore both populations follows a predator prey tendency. 	
<ul style="list-style-type: none"> • Case 2 - Tumor cell extinction: Tumor cell population decays quickly at the beginning of the simulation, and goes below 1 (blue line), therefore this population disappears from the simulation. For this case, the Effector cells achieve an equilibrium value close to the 4% of the initial value. 	
<ul style="list-style-type: none"> • Case 3 - Effector cell extinction: Effector cell population decays below 1 (red line), and therefore this population disappears from the simulation. This phenomenon only appears a few times along the different runs, for those simulations with higher scale factor values. 	

The first case deals with the pattern defined by the SDS outcome, and the other two cases are alternative results obtained through this ABS model, due to its non-deterministic effects and the scale factor values. To evaluate the outcomes of different simulations, the following points are analyzed: *i)* convergence ratio i.e., ratio of converged simulations against total number of runs (only those simulations with the same pattern as the SDS numerical solution will be considered as converged); *ii)* scattering i.e., the scatter of each single simulations against the

mean value; *iii*) mean value that is the comparison of the mean value of all the simulations performed (converged and not converged) against the SDS numerical solution; *iv*) machine resources i.e., the time necessary to get the final solution (500 runs). Taking into account these values, the following conclusions can be extracted from the simulations. Convergence ratio increases when the size of the scale factors decreases, that is, when the non-dimensional cell population increases. This behavior is well understood, as the stochastic effects are more relevant when the agent population is reduced. Based on SDS solution, expected outcome from the ABS is the predator-prey tendency (Case 1, Table 4), and all the cases converge to this solution when the size of the scale factors are $E_0=T_0=10^2$ cells. When the scale factors increase, and therefore the cell population decreases, the number of cases in which the non-dimensional tumor cell population is extinct, increases (Case 2, Table 4). In fact, if the scale factor is too high ($E_0=T_0=10^5$ cells), the effect of stochastic effect is relevant, that appears a not expected case in which, the effector cell population disappears (Case 3, Table 4). When the non-dimensional cell population decreases, and then the stochastic effects becomes predominant, scatter of the simulations increases with the size of the scaling factors. It is worth mentioning that, even the scatter for the curves increases, the frequency of the peaks for both non-dimensional populations (tumor and effector cells) is almost equal for all the simulation. This can be considered as the root cause for the scattering point at which the tumor cell populations start to increase after the initial decay, which is highly dependent of the stochastic effect. At this point the non-dimensional tumor cell population reach its minimum. Mean value is closer to the SDS solution when the scaling factors are lower. This fact is linked with the two previous points, because the not converged solutions and the scattering of the simulation are the main rationales for the adjustments of the mean value to the SDS numerical solution. Machine resources increases when the scale factors are lower. This is because, for the ABM, the number of computational operations increases with the number of agents in each population, and having lower scale factors imply to solve a problem with a high number of agents. Figure 5 and Figure 6 also capture the effect, for each scale factor, of modifying the scale factor for the time value. The effect of this scale factor can be observed by means of direct comparison between both, left and right, columns of plots, in the figures. Right column represents a low time scale factor, and therefore it is necessary to perform more non-dimensional time steps to get the same non-dimensional cell population pattern. These figures show that, for a given cell population scale factor, a reduction in the time scale factor allows to have a more accurate mean value, by means of reducing the scattering of the solution. This conclusion can be appreciated for those cases with a lower value of the cell population scale factor. For this reason, a dedicated study was performed comparing three times scale factors, and the results are depicted in Figure 7. As this figure shows, the accuracy of the results increases with the reduction of the time scale factor. The rationale for this behavior is associated with the discrete nature of the ABS model, because a reduction of the time scale factor is equivalent to a reduction of the time step of the model, and therefore it implies that the transition rates values are refreshed more frequently, because these rates are kept constant during the time step, but updated at each time step, and therefore

the final solution is closer to the SDS outcome. It should be pointed out that, during this performance analysis, the time step parameter of the ABS algorithm has been kept constant, in order to analyze only the effect of the time scale factor.

Table 5 shows the comparison between the main parameters of each simulation outcome: convergence ratio i.e., ratio of converged simulations against total number of runs (only those simulations with the predator-prey pattern is considered as converged); machine time that is the average time needed to obtain each individual simulation in a standard quad core PC; tumor RSS that represents the non-dimensional residual sum of squares between the mean value of the tumor cell population for all the runs in each scenario and the SDS curve; effector RSS that represents the non-dimensional Residual Sum of Squares between the mean value of the effector cell population for all the runs in each scenario, and the SDS curve. Both RSS values have been calculated by means of the following equation:

$$RSS = \frac{\sum_{i=1}^n \frac{(\bar{x}_i - SDS_i)^2}{SDS_i}}{n} \quad (9)$$

where \bar{x}_i represents the mean value at timestep i ; SDS_i represents the SDS solution value at timestep i . n represents the number of time steps.

TABLE V. MAIN OUTCOME COMPARISON BETWEEN THE 12 SCENARIOS EVALUATED

ID	Time factor	Scale factor	CPU Time [sec]	% of convergence	Tumour RSS	Effector RSS
#1	1	10^5	37	5.0	1.27	0.76
#2		10^4	37	46.0	0.61	0.52
#3		10^3	38	99.6	1.22	0.23
#4		10^2	59	100.0	0.93	0.24
#5	2	10^5	73	3.9	1.53	0.76
#6		10^4	74	39.0	0.42	0.43
#7		10^3	74	99.0	0.46	0.10
#8		10^2	105	100.0	0.32	0.10
#9	4	10^5	131	3.9	0.84	0.75
#10		10^4	139	27.2	0.53	0.38
#11		10^3	137	95.6	0.24	0.05
#12		10^2	191	100.0	0.13	0.04

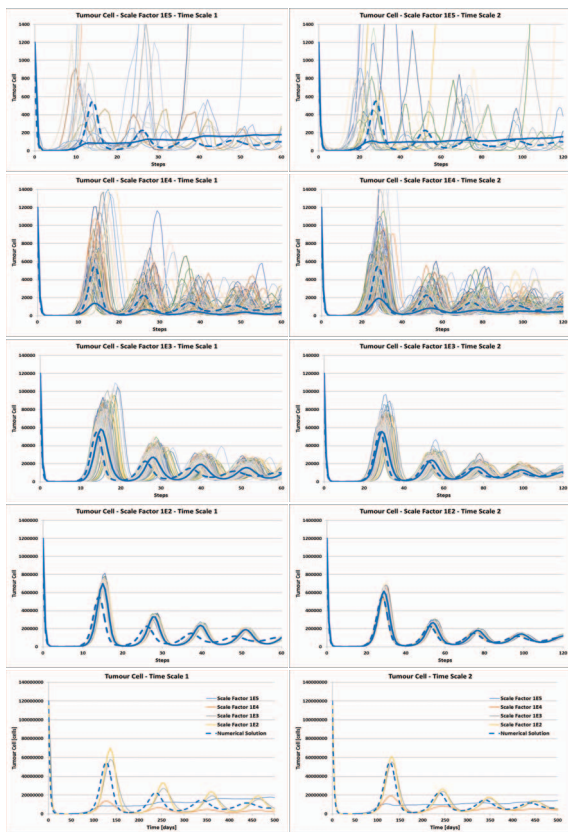


Figure 5. Effector cells population evolution.

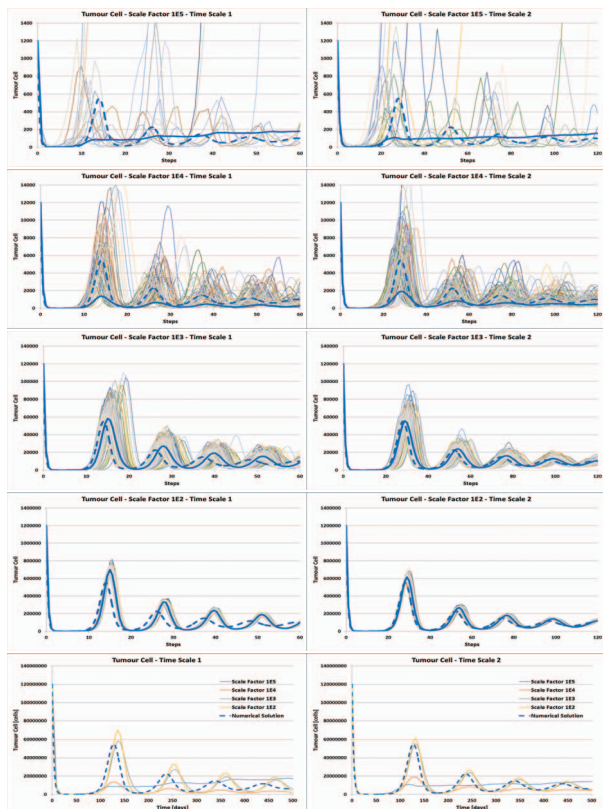


Figure 6. Tumor cells population evolution.

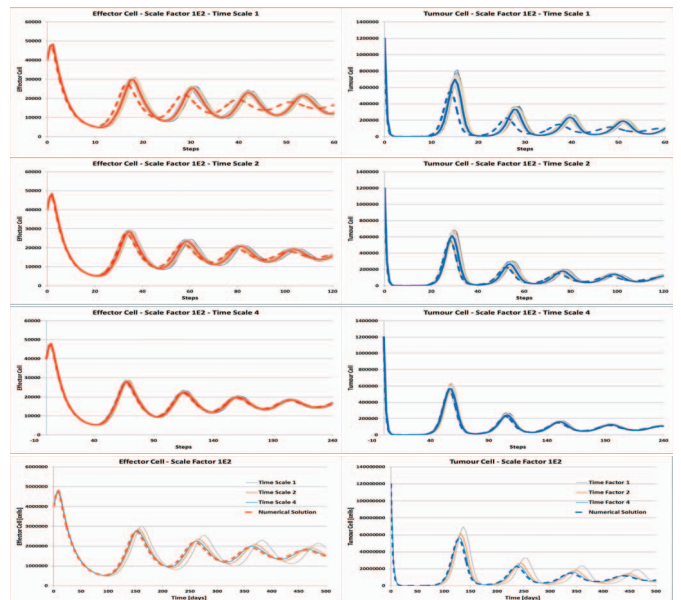


Figure 7. Effector and Tumor cells population evolution for different time scales.

IV. CONCLUSIONS

Immune system processes can be modelled through different simulation approaches. The SDS and the ABS techniques are considered two of the most effective techniques to reach this goal. Whilst SDS provides deterministic outcome, obtained generally through solving a set of differential equations, ABS allows the simulation of complex systems, through the definition of simple interactions among agents involved in the process, providing a perspective of the global behavior of the system. Due to the emergent order created from the individual behavior, ABS deliver additional information in comparison with the SDS, being this point its key characteristic. Process to create an ABS modelling from a given SDS have been explored within a lot of documentation, but influence of initial adjustment of the SDS parameters, and therefore the ABS transition rates, have not been mentioned before. SDS equations can be non-dimensionalized to simplify them and to perform a deeper analysis of the influence of each parameter in the final solution. Non-dimensional parameters are not fixed, and they can be chosen to adjust the scale of the non-dimensional solution. Once the non-dimension differential equations are solved, physical solution can be recovered to analyze the real behavior of the system. This non-dimensional analysis performed with the SDS parameters can be translated into a ABS model, by means of adjusting the transition rates values, then reducing the number of agents involved in the simulation. This parameter adjustment, shown as a non-dimensional scale factor adjustment, is a key point to ensure proper ABS behavior. It allows to find the same solution of the SDS system, achieving a compromise solution between the ABS simulations constraints (discrete number of agents and stochastic simulation) and computer resources. This study confirms the possibility of modeling a real system through two different approaches, SDS and ABS, obtaining the same output, by means of a proper adjustment of the parameters involved in the ABS modeling. An additional study of parameters sensitivity has been performed to understand the influence of them in the

final outcome, optimizing computer resources without losing accuracy in the ABS output.

ACKNOWLEDGMENT

We wish to thank Immunotek, SL and the Spanish Department of Science at MINECO for supporting the research of the Immunomedicine group through grants SAF2006:07879, SAF2009:08301 & BIO2014:54164-R to PAR.

REFERENCES

- [1] M.J. Smyth, D.I. Godfrey, J.A. Trapani, "A fresh look at tumor immunosurveillance and immunotherapy," *Nat Immunol.*, vol. 2, pp. 293-299, 2001
- [2] A. Ortega-Gomez, M. Perretti, O. Soehnlein, "Resolution of inflammation: an integrated view," *EMBO Mol Med.*, vol. 5, pp. 661-674, 2013
- [3] N.M. Vaz, G.C. Ramos, V. Pordeus, C.R. Carvalho, "The conservative physiology of the immune system. A non-metaphoric approach to immunological activity," *Clin Dev Immunol.*, vol. 13, pp. 133-142, 2006
- [4] P.A. Morel, "Mathematical modeling of immunological reactions," *Front Biosci.*, vol. 3, pp. d338-337, 1998
- [5] A. Borshchev, A. Filippov, "From System Dynamics and Discrete Event to Practical Agent Based Modeling: Reasons, Techniques, Tools.," in: K. Kennedy, G.W. Winch, R.S. Langer, J.I. Rowe, M.Y. Yanni (Eds.) *The 22nd International Conference of the System Dynamics Society*, Wiley, Oxford, England, 2004
- [6] F. Chiacchio, M. Pennisi, G. Russo, S. Motta, F. Pappalardo, "Agent based modeling of the immune system: NetLogo, a promising framework," *BioMed Research International*, vol. 2014 article ID: 907171, 2014
- [7] F. Pappalardo, M. Pennisi, A. Ricupito, F. Topputo, M. Bellone, "Induction of T cell memory by a dendritic cell vaccine: a computational model," *Bioinformatics*, vol. 30(13), pp. 1884-1891, 2014
- [8] F. Castiglione, F. Pappalardo, C. Bianca, G. Russo, S. Motta, "Modeling biology spanning different scales: An open challenge," *BioMed Research International*, vol. 2014, article ID: 902545, 2014
- [9] M.A. Burke, B.F. Morel, T.B. Oriss, J. Bray, S.A. McCarthy, P.A. Morel, "Modeling the proliferative response of T cells to IL-2 and IL-4," *Cell Immunol.*, vol. 178, 42-52, 1997
- [10] R. Fernandez-Botran, V.M. Sanders, T.R. Mosmann, E.S. Vitetta, "Lymphokine-mediated regulation of the proliferative response of clones of T helper 1 and T helper 2 cells," *J Exp Med.*, vol. 168, 543-558, 1988
- [11] H.Y. Lee, D.J. Topham, S.Y. Park, J. Hollenbaugh, J. Treanor, T.R. Mosmann, X. Jin, B.M. Ward, H. Miao, J. Holden-Wiltse, A.S. Perelson, M. Zand, H. Wu, "Simulation and prediction of the adaptive immune response to influenza A virus infection," *J Virol.*, vol. 83, pp. 7151-7165, 2009
- [12] D. Wodarz, A.R. Thomsen, "Effect of the CTL proliferation program on virus dynamics," *Int Immunol.*, vol. 17, pp. 1269-1276, 2005
- [13] R.J. De Boer, A.S. Perelson, "Quantifying T lymphocyte turnover," *J Theor Biol.*, vol. 327, pp. 45-87, 2013
- [14] D. Fouchet, R. Regoes, "A population dynamics analysis of the interaction between adaptive regulatory T cells and antigen presenting cells," *PLoS One*, vol. 3, doi: 2310.1371/journal.pone.0002306, 2008
- [15] V.A. Kuznetsov, I.A. Makalkin, M.A. Taylor, A.S. Perelson, "Nonlinear dynamics of immunogenic tumors: parameter estimation and global bifurcation analysis," *Bull Math Biol*, vol. 56, 295-321, 1994
- [16] A.G. Lopez, J.M. Seoane, M.A. Sanjuan, "A validated mathematical model of tumor growth including tumor-host interaction, cell-mediated immune response and chemotherapy," *Bull Math Biol.*, vol. 76, pp. 2884-2906, 2014
- [17] Y. Louzoun, C. Xue, G.B. Lesinski, A. Friedman, "A mathematical model for pancreatic cancer growth and treatments," *J Theor Biol.*, vol. 351, pp. 74-82, 2014
- [18] J.D. Serman, "System dynamics modeling: Tools for learning in a complex world," *California management review*, vol. 43, pp. 8-25, 2001
- [19] V.A. Folcik, G. Broderick, S. Mohan, B. Block, C. Ekbote, J. Doolittle, M. Khoury, L. Davis, C.B. Marsh, "Using an agent-based model to analyze the dynamic communication network of the immune response," *Theor Biol Med Model.*, vol. 8:1, 10.1186/1742-4682-1188-1181, 2011
- [20] N. Schieritz, P.M. Milling, "Modeling the forrest or modeling the trees: A comparison of system dynamics and agent based simulation," in: *proceedings of the XXI International Conference of the System Dynamics society*, 2003
- [21] M. Holcombe, S. Adra, M. Bicak, S. Chin, S. Coakley, A.I. Graham, J. Green, C. Greenough, D. Jackson, M. Kiran, S. MacNeil, A. Maleki-Dizaji, P. McMinn, M. Pogson, R. Poole, E. Qwarnstrom, F. Ratnieks, M.D. Rolfe, R. Smallwood, T. Sun, D. Worth, "Modelling complex biological systems using an agent-based approach," *Integr Biol (Camb)*, vol. 4, pp. 53-64, 2012
- [22] S. Forrest, C. Beauchemin, "Computer immunology," *Immunol Rev.*, vol. 216, pp. 176-197, 2007
- [23] A. Casal, C. Sumen, T.E. Reddy, M.S. Alber, P.P. Lee, "Agent-based modeling of the context dependency in T cell recognition," *J Theor Biol.*, vol. 236, pp. 376-391, 2005
- [24] G. Bogle, P.R. Dunbar, "On-lattice simulation of T cell motility, chemotaxis, and trafficking in the lymph node paracortex," *PLoS One.*, vol. 7, doi: 45210.41371/journal.pone.0045258, 2012
- [25] J. von Eichborn, A.L. Woelke, F. Castiglione, R. Preissner, "VacImm: simulating peptide vaccination in cancer therapy," *BMC Bioinformatics.*, vol. 14:127, doi: 10.1186/1471-2105-1114-1127, 2013
- [26] F. Celada, P.E. Seiden, "A computer model of cellular interactions in the immune system," *Immunol Today.*, vol. 13, pp. 56-62, 1992
- [27] J. Mata, M. Cohn, "Cellular automata-based modeling program: synthetic immune system," *Immunol Rev.*, vol. 216, pp. 198-212, 2007
- [28] V.A. Folcik, G.C. An, C.G. Orosz, "The Basic Immune Simulator: an agent-based model to study the interactions between innate and adaptive immunity," *Theor Biol Med Model.*, vol. 4, pp. 39, 2007
- [29] C.M. Macal, "To agent-based simulation from system dynamics," in: *2010 Winter Simulation Conference*, 2010
- [30] G.P. Figueredo, U. Aickelin, Investigating immune system aging: System dynamics and agent-based modelling, in: *Proceedings of the Summer Computer Simulation Conference*, 2010
- [31] P.S. Kim, D. Levy, P.P. Lee, "Modeling and simulation of the immune system as a self-regulating network," *Methods Enzymol.*, vol. 467, pp. 79-109, 2009
- [32] G.P. Figueredo, U. Aickelin, "Comparing System Dynamics and Agent-Based Simulation for Tumour Growth and its Interactions with Effector Cells," in: *International Summer Computer Simulation Conference 2011*, 2011, pp. 15-22
- [33] H. Siu, E.S. Vitetta, R.D. May, J.W. Uhr, "Tumor dormancy. I. Regression of BCL1 tumor and induction of a dormant tumor state in mice chimeric at the major histocompatibility complex", *J Immunol*, vol. 137, pp. 1376-1382, 1986
- [34] J.W. Uhr, T. Tucker, R.D. May, H. Siu, E.S. Vitetta, "Cancer dormancy studies of the murine BCL1 lymphoma," *Cancer Research*, vol. 51, pp. 5045s-5053s, 1991
- [35] K.A. Krolick, P.C. Isakson, J.W. Uhr, E.S. Vitetta, "BCL1, a murine model for chronic lymphocytic leukemia: use of the surface immunoglobulin idiotype for the detection and treatment of tumor," *Immunol Rev*, vol. 48, pp. 81-106, 1979
- [36] V.A. Kuznetsov, "A mathematical model for the interaction between cytotoxic lymphocytes and tumour cells. Analysis of the growth, stabilization and regression of the B cell lymphoma in mice chimeric with respect to the major histocompatibility complex," *BioMedical Science*, vol. 2, pp. 465-476, 1991
- [37] V.A. Kuznetsov, V.P. Zhivoglyadov, L.A. Stepanova, "Kinetic approach and estimation of the parameters of cellular interaction between the immunity system and a tumor," *Arch Immunol Ther Exp (Warsz)*, vol. 41, pp. 21-31, 1993
- [38] G.P. Figueredo, P.O. Siebers, M.R. Owen, J. Repts, U. Aickelin, "Comparing stochastic differential equations and agent-based modelling and simulation for early-stage cancer," *PLoS One*, vol. 9, e95150, 2014